Protein Expression and Purification 101 (2014) 115–120

Contents lists available at ScienceDirect

Protein Expression and Purification

journal homepage: www.elsevier.com/locate/yprep

# A simple strategy for the purification of native recombinant full-length human RPL10 protein from inclusion bodies

Larissa M. Pereira [a], Luana R. Silva [a], Joseane F. Alves [a], Nélida Marin [b], Flavio Sousa Silva [a], Ligia Morganti [a], Ismael D.C.G. Silva [c], Regina Affonso [a,c,*]

[a] Biotechnology Department, IPEN-CNEN, SP, Brazil
[b] Biochemistry Department, IQUSP, Brazil
[c] Molecular Gynaecology Laboratory, UNIFESP, SP, Brazil

ARTICLE INFO

*Article history:*
Received 14 May 2014
Available online 23 June 2014

*Keywords:*
Inclusion bodies
Soluble protein
Binding zinc ions
Correct folding

ABSTRACT

The L10 ribosomal protein (RPL10) plays a role in the binding of the 60 S and 40 S ribosomal subunits and in mRNA translation. The evidence indicates that RPL10 also has multiple extra-ribosomal functions, including tumor suppression. Recently, the presence of RPL10 in prostate and ovarian cancers was evaluated, and it was demonstrated to be associated with autistic disorders and premature ovarian failure. In the present work, we successfully cloned and expressed full-length human RPL10 (hRPL10) protein and isolated inclusion bodies containing this protein that had formed under mild growth conditions. The culture produced 376 mg of hRPL10 protein per liter of induced bacterial culture, of which 102.4 mg was present in the soluble fraction, and 25.6 mg was recovered at approximately 94% purity. These results were obtained using a two-step process of non-denaturing protein extraction from pelleted inclusion bodies. We studied the characteristics of this protein using circular dichroism spectroscopy and by monitoring the changes induced by the presence or absence of zinc ions using fluorescence spectrometry. The results demonstrated that the protein obtained using these non-conventional methods retained its secondary and tertiary structure. The conformational changes induced by the incorporation of zinc suggested that this protein could interact with Jun or the SH3 domain of c-yes. The results suggested that the strategy used to obtain hRPL10 is simple and could be applied to obtaining other proteins that are susceptible to degradation.



## Introduction

The ribosomal protein L10 (RPL10),[1] which is also called QM protein, is associated with the ribosomes in the rough endoplasmic reticulum. In yeast, RPL10 is one of the last proteins to assemble onto the nascent 60 S subunit. RPL10 is one of three proteins that exchange binding to the 60 S ribosomal subunit [1], and RPL10 it allows the 60 S subunit to associate with the 40 S subunit and enables mRNA translation [1]. RPL10 is well conserved from yeast to mammals, suggesting that this factor is essential for basic cellular functions [2]. Evidence indicates that RPL10 has multiple extra-ribosomal functions in addition to its housekeeping role during protein synthesis [3,4].

The literature suggests that the RPL10 protein is a tumor suppressor. Jif-1, a chicken ortholog of human RPL10 (hRPL10), was reported to interact with the transcription factor c-Jun, thus preventing c-Jun from activating genes containing AP-1 binding sites [3]. The interaction between Jif-1 and c-Jun occurs via binding of Jif-1/hRPL10 to the leucine zipper region of c-Jun, which is controlled by hRPL10 phosphorylation [3,5]. The transport of hRPL10 into the nucleus is mediated by presenilin 1 [6]. hRPL10 has been demonstrated to interact with several Src family kinases such as c-yes, and thus it may participate in the signal transduction processes of these kinases that play roles in many intracellular functions, including cell stability, division, proliferation, migration and differentiation [7,8].

* Corresponding author at: Biotechnology Centre, IPEN-CNEN, Av. Prof. Lineu Prestes, 2242, Cidade Universitária, 05508-900 São Paulo, Brazil. Tel.: +55 21 11 31339707; fax: +55 11 31339709.
*E-mail address:* reginaffonso@yahoo.com.br (R. Affonso).

[1] *Abbreviations used:* hRPL10, human ribosomal protein L10; pfRPL10, *Pincatada fucata* ribosomal protein L10; GFP, green fluorescent protein; mRNA, messenger RNA; IBs, inclusion bodies; LB, Luria Broth; SDS, sodium dodecyl sulfate; PAGE, polyacrylamide gel electrophoresis; CD, circular dichroism; RPM, revolutions per minute; EDTA, ethylenediaminetetraacetic acid; sp1 and sp2, first and second supernatants after sonication; F, amino acid phenylalanine; G, amino acid glycine; K, amino acid lysine; Q, amino acid glutamine; R, amino acid arginine; W, amino acid tryptophan.

http://dx.doi.org/10.1016/j.pep.2014.06.003
1046-5928/

The tumor suppressor activity of hRPL10 was first detected using a subtractive hybridization assay conducted utilizing a Wilms' tumor cell line [2]. The expression of hRPL10 was also recently evaluated during the early stage of the development of prostate cancer and in ovarian cancer [9,10]. In addition, hRPL10 has been associated with autistic disorders [11,12] and premature ovarian failure [13].

The hRPL10 protein consists of 214 amino acid residues. It is not glycosylated, which facilitates its expression in bacterial systems; however, the bacterial expression of full-length hRPL10 has not been achieved. The crystal structure of the core domain region (Phe34-Glu182) of hRPL10 has been described in the literature, but hRPL10 has not been subjected to comprehensive structural studies, most likely due to the occurrence of protein aggregation and fragmentation during the purification procedure [15].

Expressing hRPL10 protein in inclusion bodies (IBs) may be a good strategy for obtaining material for structural analysis because up to 90% of the proteins in IBs are recombinant proteins. Moreover, IBs can be easily separated from cellular debris using simple procedures that limit proteolysis [16,17]. IBs were long considered as deposits of inactive accumulated recombinant proteins. Nevertheless, several authors have demonstrated that IBs containing a high percentage of correctly folded protein can be extracted under non-denaturing conditions in a biologically active form without applying any renaturation steps [17].

In the present study, hRPL10 protein was expressed and incorporated into IBs in bacteria that were cultivated under mild growth conditions. The culture produced 376 mg of hRPL10 protein per liter of induced bacterial culture, of which 105.6 mg was soluble, from which 25% was recovered as nearly pure hRPL10. The full-length hRPL10 attained the correct secondary and tertiary structure, as was confirmed by circular dichroism spectroscopy and fluorescence spectrometry, respectively. Analyses of hRPL10 following zinc incorporation and chelation showed that the addition and removal of this ion led to changes in its conformation.

## Materials and methods

### *Cloning and expression of the recombinant protein*

The cDNA encoding human RPL10 was cloned into the p1813 vector (Fig. 1a), sequenced and expressed in *Escherichia coli* HB2151. The transformed *E. coli* HB2151 containing the p1813_hRPL10 plasmid was grown in LB medium (10 g/L Tryptone, 5 g/L yeast extract, and 10 g/L NaCl) supplemented with kanamycin (50 μg/mL) at 37 °C while shaking at 200 rpm. When the $OD_{600}$ reached 0.4–0.8, the cells were induced with 0.5 mM IPTG for 16 h at 18 °C, 25 °C, 30 °C or 37 °C while shaking at 150 rpm. Then, the cultures were centrifuged at 1900×*g* for 10 min at 4 °C and the pellets were processed or stored at −20 °C [18].

### *hRPL10 protein isolation*

All of the pellets were processed using the same methodology. The pellet from the induced culture, 7712 mg of wet weight of cells, was suspended in 256 mL of 20 mM Tris–HCl buffer, pH 7.5. The suspension was sonicated seven times for 30 s each on ice and then was centrifuged at 9500×*g* for 10 min at 4 °C. The supernatant (designated sp1) was stored on ice. The pellet was suspended in 128 mL of the same buffer, sonicated once and centrifuged at 9500×*g* for 10 min at 4 °C. The second supernatant (designated sp2) was also stored on ice [19]. The induced cultures, non-induced cultures and soluble fractions were analyzed using 12% SDS–PAGE [20] and Western blotting [21].

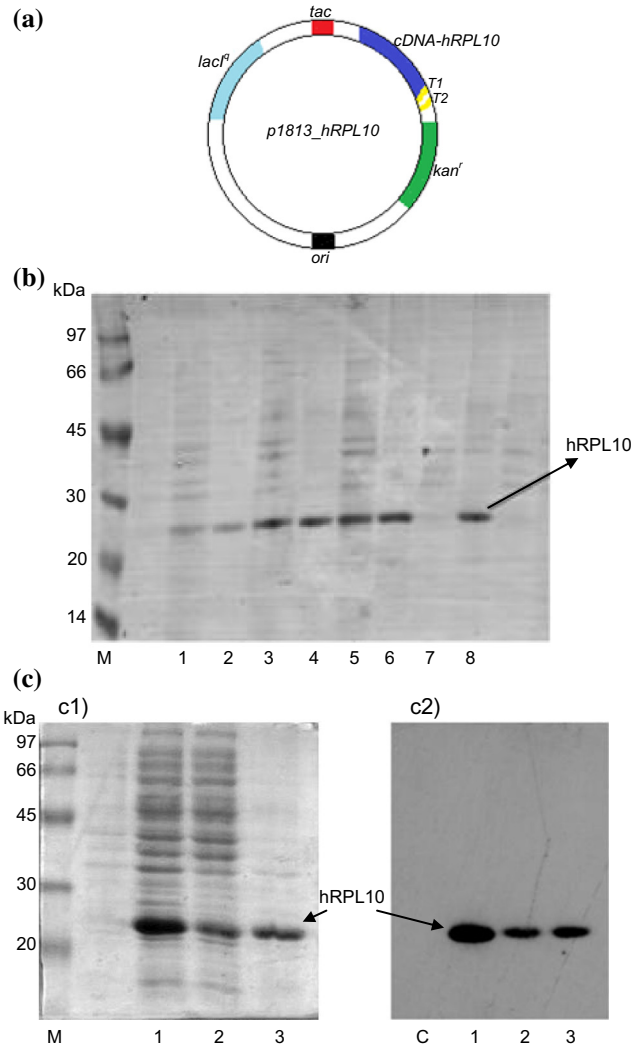


**Fig. 1.** (a) Schematic representation of the p1813_hRPL10 vector showing the location with a description of its elements: *ori* (replication origin); *tac* (transcriptional promoter); *kan*$^r$ (kanamycin resistance gene); hRPL10 (cDNA of the hRPL10 protein); *lacI*$^q$ (tac promoter inhibitor); and *T1* and *T2* (transcription terminators). (b) Polyacrylamide gel of samples of cultures of p1813_hRPL10-transformed *E. coli* that were induced for 16 h at different temperatures using IPTG. Lane M, protein molecular weight; markers. Supernatants and pellets: lanes 1 and 2, culture induced at 18 °C; lanes 3 and 4, culture induced at 25 °C; lanes 5 and 6, culture induced at 30 °C; lanes 7 and 8, culture induced at 37 °C. (c) Characterization of hRPL10 protein by SDS–PAGE (c1) and Western blotting (c2). The samples were obtained from a culture induced at 25 °C. Lane M, protein markers; lane 1, induced culture; lane 2, supernatant 1 (sp1); lane 3, supernatant 2 (sp2); lane C, non-induced culture.

### *SDS–PAGE and Western blotting analysis*

Samples of *E. coli* that were transformed with p1813_hRPL10 and cultured at different induction temperatures were analyzed. The SDS–PAGE (sodium dodecyl sulfate polyacrylamide gel electrophoresis) analyses were conducted using a 12% denaturing polyacrylamide gel and staining with Coomassie Blue. For Western blotting analysis, the proteins separated in the polyacrylamide gel were transferred to a nitrocellulose membrane. The membrane was incubated with polyclonal rabbit anti-RPL10 antiserum (Santa Cruz) at a 1:500 dilution and then incubated with horseradish-peroxidase-conjugated anti-rabbit IgG (1:2000 dilution). An ECL Advance Western Blotting Detection Kit (GE) was used for visualization.

*Protein quantification*

The protein concentration was determined using the Bradford method [22] (Bio-Rad Laboratories Inc., Hercules, CA, USA), and the concentration of hRPL10 in the samples was determined by scanning the SDS–PAGE gel and using Image J software.

*Circular dichroism (CD) spectroscopy*

The sp2 fraction of the hRPL10 protein (at 50 μM in 20 mM Tris–HCl buffer, pH 7.5) was analyzed using circular dichroism spectroscopy. Far-ultraviolet CD spectra were obtained using a Jasco J-810 (Japan) spectropolarimeter with a 0.1-cm light path at 20 °C. The ellipticity was recorded from 190 to 260 nm, and the scan was repeated four times. The values obtained using reference samples lacking protein were subtracted in all cases. The profiles were obtained using the CDNN program [23].

*Fluorescence spectroscopic analysis*

The tertiary structure of hRPL10 protein in the sp2 fraction (50 μM) was analyzed. The data were obtained at between 300 and 430 nm using an AB2 Luminescence Spectrometer. Analyses of the effect of $Zn^{2+}$-ion incorporation were conducted at $ZnCl_2$ concentrations of 0 μM, 0.25 μM, 1.25 μM, 6.25 μM and 31.25 μM, with an incubation period of 30 min at 25 °C. The $Zn^{2+}$ ions were removed by adding $Na_4EDTA$ tetrahydrate (EDTA) pH 8.0, to the hRPL10 samples containing 31.25 μM $ZnCl_2$; the final EDTA concentrations were 50 mM and 100 mM.

## Results and discussion

We first expressed hRPL10 in the bacterial periplasm using the pET26 vector (Novagen). This expression system yielded hRPL10 at a concentration of 130 mg per liter of induced bacterial culture. hRPL10 was extracted using the osmotic-shock method [24]. However, during purification using immobilized metal-ion affinity [His Trap FF, (GE)], cationic exchange [HiTrap SP Sepharose (GE)] or gel-filtration chromatography [SEC (GE)], the protein did not bind or was degraded (data not shown). Upon cytoplasmic expression, aggregated hRPL10 was identified in sub-classes of IBs with different compositions, and these aggregates were protease resistant [25].

*Cloning and expression of recombinant hRPL10 protein*

The p1813 vector was chosen to express the hRPL10 protein because this vector was derived from pTug A, which can express intracellular recombinant proteins at levels as high as 250 mg per liter of bacterial culture [26]. hRPL10 protein expression was well above the expected level, reaching an average of 300 mg of hRPL10 per liter of bacterial culture in inclusion bodies following culture at 37 °C. When these IBs were treated with urea- or guanidine-containing buffers, the hRPL10 protein appeared to have most likely degraded, as previously described by Nishimura et al. [15].

The formation of inclusion bodies in recombinant expression systems depends on the balance between aggregated and soluble proteins. The aggregation reaction is generally favored at higher temperatures because of their effect on hydrophobic interactions [27]. The direct consequences of temperature reduction include the partial elimination of heat-shock proteases that are induced under overexpression conditions [27] and the inhibition of DNA replication, transcription and translation, which reduces the growth rate of *E. coli* [25]. In addition, experiments were performed using a reduced rate of rotary shaking to decrease the aeration of the culture medium and thus decrease the rate of bacterial growth [28]. In this study, we cultivated *E. coli* at reduced temperatures and with shaking of 150 rpm for 16 h.

The results of hRPL10 expression at 18 °C, 25 °C, 30 °C and 37 °C are presented in Fig. 1b. Soluble hRPL10 protein was produced at 18 °C, 25 °C and 30 °C (Fig. 1b, lanes 1, 3 and 5), although the production rate at 18 °C was very low.

Table 1 shows the amount of protein in the cultures induced at 25 °C, 30 °C and 37 °C and that obtained in them in the soluble form. The expression of hRPL10 protein at 18 °C was not reproducible and the standard deviation was extremely high, so this result was not included in Table 1. The expression levels at 25 °C and 30 °C were very similar (376 mg and 340 mg, respectively) and were higher than that at 37 °C (272 mg). Despite the inhibition of elements of the bacterial replication system due to reducing the expression temperature, the low shaking rate and 16-h induction period allowed for higher expression of the protein of interest. The amount of hRPL10 produced at 25 °C was approximately 39% greater than that produced at 37 °C.

*Isolation of hRPL10 protein*

The first supernatant obtained after sonicating the induced culture (sp1) contained a large quantity of hRPL10; however, this sample also contained a large amount of bacterial proteins. Purification of hRPL10 protein from the sp1 fraction was unsuccessful. This protein degraded during size-exclusion chromatography [Superdex 75 (GE)], as previously described by Nishimura et al. [15], and it failed to bind to the matrix during ion-exchange chromatography [SP Sepharose XL (GE)].

As previously reported for a wide range of proteins, the production of IBs at a low temperature rather than a high temperature results in a higher concentration of relatively pure protein sequestered in proteolysis-resistant aggregates, such that the native protein of interest can be recovered using the appropriate procedure [29]. The pellet of the first sonicate was suspended to extract the remaining soluble hRPL10 protein. This strategy was effective in obtaining nearly pure soluble hRPL10 protein (Fig. 1c1, lane 3).

The yield of hRPL10 protein from a culture grown at 25 °C was 376 mg (Table 1); 25.6 mg of this protein was recovered in the sp2 fraction at approximately 94% purity and this concentration was sufficient to allow structural characterization using circular dichroism spectroscopy and fluorescence spectroscopy. Fig. 1c shows the results of PAGE of the induced culture sample and the sp1 samples (lanes 1 and 2, respectively), which contained significant amounts of impurities. Lane 3 in Fig. 1c represents the sp2 sample of hRPL10, which had very little contaminating protein. Fig. 1c2 shows a Western blotting of the same samples. In this figure, lane C was a sample from the non-induced culture that did not contain hRPL10 and lanes 1, 2 and 3 were samples containing hRPL10. The concentrations in the sp1 and sp2 samples were similar, and the same volume of each sample was applied.

The low growth rate achieved by decreasing the rotational rate of the culture and maintaining the temperature at between 25 °C and 30 °C allowed for the formation of IBs containing the largest amount of native protein, 105.6 mg of hRPL10, corresponding to 27% of the total hRPL10 produced. The native protein was extracted in almost pure form from the second pellet, with 25% recuperated.

*Circular dichroism*

Circular dichroism (CD) spectroscopy is the ideal technique for determining the secondary structure of proteins; therefore, this technique was used to determine the secondary structure of hRPL10 in the sp2 fractions. The CD analyses revealed that the

**Table 1**
Quantities of hRPL10 that was produced in induced cultures (IC) grown at 25 °C, 30 °C and 37 °C and that was observed in the following samples: sp1 (supernatant of pellet 1) and sp2 (supernatant of pellet 2). These amounts were obtained from induced cultures containing 7712 mg of biomass (wet weight).

| Induction temperature | | Total protein (mg) | Target protein (mg) | Content of hRPL10 (%) |
|---|---|---|---|---|
| 25 °C | IC | 1331 | 376 | 28 |
| | sp1 | 384 | 76.8 | 20 |
| | sp2 | 0.27 | 25.6 | 94 |
| 30 °C | IC | 1152 | 340 | 30 |
| | sp1 | 409.6 | 89.6 | 22 |
| | sp2 | 27.1 | 24.4 | 90 |
| 37 °C | IC | 1382 | 272 | 20 |
| | sp1 | – | – | – |
| | sp2 | – | – | – |

sp2 fractions obtained from cultures induced at 25 °C and 30 °C contained hRPL10 protein with the correct secondary structural conformation. Fig. 2a shows the spectral peaks of protein expressed at 25 °C and 30 °C: the maximal peaks occurred at 194.5 and 194 nm, respectively, and the minimal peaks occurred were at 211.5 and 212.5 nm, respectively. The lack of a well-defined maximum and minimum between these sets of peaks indicated the presence of α-helical structures because the expected values for β-sheets are 198 and 215 nm. In fact, the crystal structure of the truncated form that was presented in the literature demonstrated the presence of six β-sheets between two external α-helices [14].

Structural analysis of the soluble protein fraction by CD demonstrated that this protein consisted of 25% alpha helices and 42% beta sheets (Table 2), suggesting that the protein had the correct structure.

Low temperature culture presents the following advantages: it slows down the rates of transcription and translation, reduces the strength of hydrophobic interactions and decreases the chaperone level, which helps to prevent protein misfolding. Our results are consistent with previous analyses of GFP (green fluorescent protein) sequestration in the soluble fraction following expression at different temperatures. Vera et al. [29] observed a progressive enhancement of GFP's specific fluorescence, indicating that GFP folded correctly when produced in *E. coli* below 37 °C. In this study, the tertiary structure of hRPL10 was confirmed using fluorescence spectroscopy.

**Table 2**
Percentage of secondary structural elements in hRPL10 protein. The spectra were fitted using standard CDNN software (available at http://bioinformatik.biochemtech.unihalle.de/cd spec/cdnn).

| hRPL10 | α-Helix (%) | β-Sheet (%) | β-Turn (%) | Random coil (%) |
|---|---|---|---|---|
| Expressed at 25 °C | 25 | 23 | 19 | 41 |

The values obtained using this software can deviate between 5% and 10%.

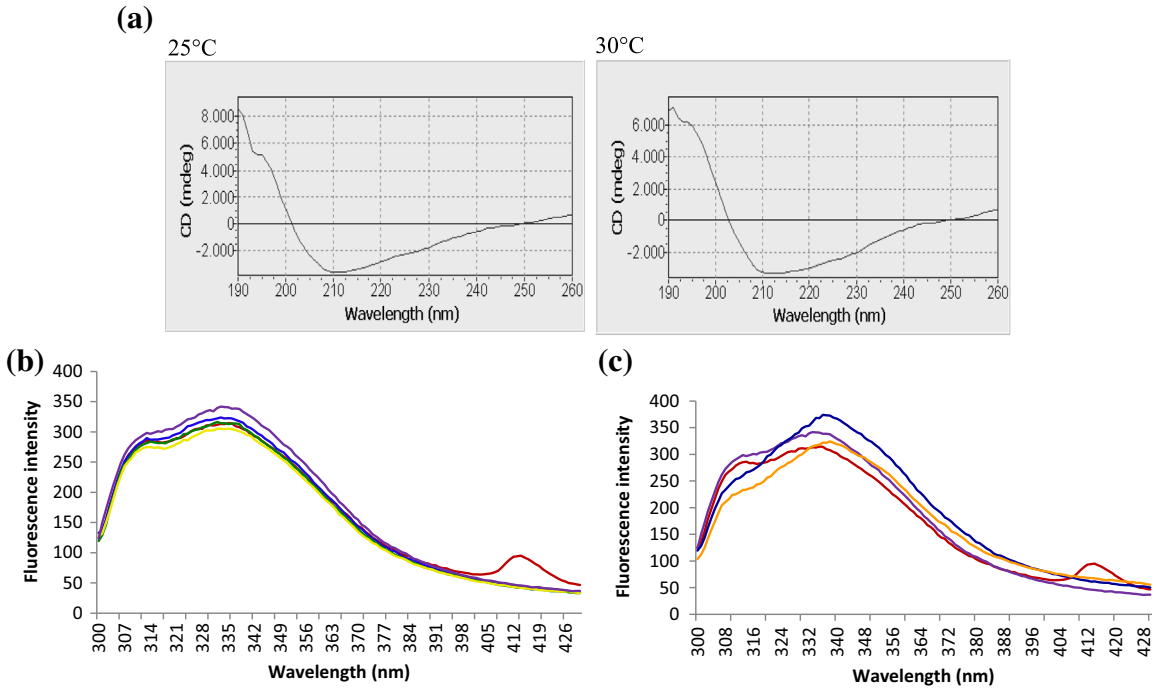


**Fig. 2.** (a) Circular dichroism analysis of the secondary structure of hRPL10 protein in the sp2 fractions of cultures that were grown at 25 °C and 30 °C. (b and c) Fluorescence emission spectral analysis of the sp2 fraction from a culture grown at 25 °C. (b) spectra after zinc-ion incorporation into the hRPL10 protein: red line, 0 μM Zn; dark blue line, 0.25 μM Zn; green line, 1.25 μM Zn; yellow line, 6.25 μM Zn; and blue line, 31.25 μM Zn. (c) Effects of the addition of EDTA to samples containing 31.25 μM $ZnCl_2$: red line, 0 μM Zn/no EDTA; blue line, 31.25 μM Zn/no EDTA; purple line, 31.25 μM $ZnCl_2$ plus 50 mM EDTA; and orange line, 31.25 μM $ZnCl_2$ plus 100 mM EDTA. (For interpretation of the references to color in this figure legend, the reader is referred to the web version of this article.)

*Fluorescence spectroscopy*

Fluorescence spectroscopy is widely used in studies of the structure and the dynamic properties of proteins that are directly related to their biological functions, such as specific binding [30].

The tertiary structure of hRPL10 protein in the sp2 fraction was evaluated using this fluorescence technique (Fig. 2b). The obtained profile is in agreement with that obtained by Zhang et al. [31] for *Pincatada fucata* RPL10 (pfRPL10), an oyster RPL10. The human protein contains two tryptophan (W) and six tyrosine (Y) residues and exhibited a maximum intrinsic fluorescence at 280 nm and an emission peak red-shifted to 335 nm (Fig. 2b, red line), similar to that obtained for pfRPL10, which contains four W and eleven Y residues.

Very recently, crystallographic studies of truncated hRPL10 demonstrated a structure with six antiparallel β-sheets and two external α-helices (β1–β2–α1–β3–β4–β5–α2–β6) [3] and the tertiary conformation that forms the cation-binding site (Fig. 3, red box). A cation-binding pocket is located at the turn between α2 and β6 of hRPL10 and residues K 156 (α2), F 159, G 161 and Q 163 (β6) are the cation-binding residues. The incorporation of the zinc atom in the α2/β6 pocket region brings these two structures closer together. One consequence of zinc incorporation was a decrease in tryptophan exposure, most likely because the indole ring of W 171 at the C-terminal part of hRPL10 is located between the R 90 and R 139 side chains, which protrude from the β3 and β5 sheets, respectively [14].

Fluorescence spectroscopic analysis of hRPL10 protein with bound zinc ions demonstrated the displacement of the maximum tryptophan-fluorescence emission from 335 to 332 nm.

This decrease in the maximum tryptophan-fluorescence emission indicated the incorporation of zinc ions by the protein. Using higher zinc concentrations of 6.25 μM and 31.25 μM did not significantly change this value, indicating that 6.25 μM most likely contained the maximum amount of zinc that the hRPL10 protein could bind. The maximum zinc concentration used by Zhang et al. [31] was 1.25 μM, whereas we used higher zinc concentrations. As shown in Fig. 2b, the intrinsic fluorescence of hRPL10 increased when the zinc concentration was increased to 31.25 μM (Fig. 2b, blue line).

The tryptophan fluorescence value we observed following zinc incorporation was different from that obtained by Zhang et al. [31]. These authors reported an increase in the value (345.5–346.5 nm), whereas we found a decrease (335–332 nm). We believe that Zhang et al. [31] found an increase in this value because pfRPL10 contains four tryptophan residues, one of which is located at residue 226 of the C-terminal region (Fig. 3, blue box). This region becomes narrower due to zinc binding and most likely leaves the fourth tryptophan residue more exposed. In the case of hRPL10, the second tryptophan of the C-terminal region, residue 209, remained between the β-sheets [14], leaving it relatively less exposed.

To confirm the zinc binding of hRPL10, we removed the zinc ions by adding EDTA. Fig. 2c shows the profile obtained following the addition of EDTA to samples containing 31.25 μM $ZnCl_2$. The EDTA concentrations were selected based on assays using increasing concentrations of EDTA including 0 mM, 0.05 mM, 0.1 mM, 1 mM, 10 mM, 50 mM and 100 mM (data not shown). The 50 mM and 100 mM concentrations were those that produced changes in the protein's conformation.

These conformational changes were detected using fluorescence spectrometry, which revealed a significant increase in the maximum tryptophan-fluorescence emission, from 333 nm to 338 nm. This increase suggested that EDTA removed the zinc ions from the hRPL10 molecules, leading to greater exposure of the tryptophan residues. The tryptophan-fluorescence emission value of 338 nm of the sample containing 100 mM EDTA was greater than the value of 335 nm of the native sample. We believe that the native protein could have already bound zinc ions that were present in the buffer, even though the buffer had been prepared using deionized water.

Zinc ions are necessary for the binding of hRPL10 to c-Jun. Although hRPL10 does not contain a leucine-zipper region, it binds to the leucine zipper of c-Jun. hRPL10 has eight cysteine residues and eight histidine residues. However, these residues do not fit the spacing patterns in known zinc-binding proteins [3]. Cysteine-rich zinc-binding motifs known as the RING-finger domain and the B-box are found in several unrelated proteins. Structural, biochemical and biological studies of these motifs have revealed that they mediate protein–protein interactions [32]. Like hRPL10, RING finger proteins may have either cytoplasmic or nuclear functions [33]. Although the amino acid sequence of hRPL10 does include the precise RING-finger motif, these domains are not yet well understood and related sequences in hRPL10 could perform their function.

We presume that the non-classical IBs that formed under the conditions of low temperature and low culture-rotational speed [28] included a large amount of hRPL10 protein existing in its native or almost correctly folded conformations, enabling the monomeric protein to be easily extracted and finally oxidized to the stable, disulfide-linked biologically active form. This hypothesis is supported by reports of several proteins that retained native-like structures within IBs [17].

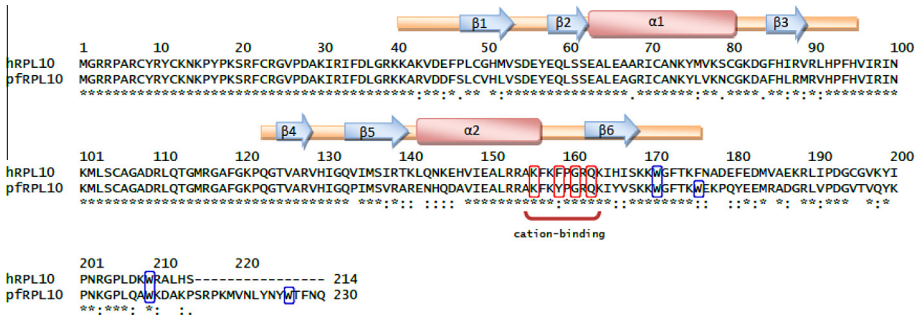


**Fig. 3.** Comparison of the structures of the human and *Pincatada fucata* RPL10 proteins. A schematic representation of the putative tertiary structure of hRPL10 is aligned with that determined forpfRPL10 (modified from Nishimura et al., 2008). The zinc-binding site between α2 and β6 is depicted in red (cation binding) and the tryptophan residues are depicted in blue, of which there as two in hRPL10 and four in pfRPL10. (For interpretation of the references to color in this figure legend, the reader is referred to the web version of this article.)

## Conclusion

We have established an efficient protocol for the expression and isolation of full-length hRPL10 protein. The results presented here suggested that this non-classical technique for extracting native hRPL10 from IBs is highly efficient, rapid and easy to perform. Obtaining this protein in the intact form is critical for studies of its structure and function, because the C-terminal region of hRPL10 (amino acid 187–214) allows its stable binding to the 60 S ribosomal subunit. Furthermore, the strategy used to obtain hRPL10 is simple and could be applied to any protein that is very susceptible to degradation [28].

## Acknowledgments

We thank Dr. Dulce E. Casarini and Mrs. Daniela Aragão from UNIFESP/EPM, the members of the Laboratório de Espectroscopia e Calorimetria – Pólo II de Alta Tecnologia (LNLS-SP) and Mrs. Karina C. de Oliveira and Dr. Patrick J. Spencer and the members of the Grupo de Hormônios from the Centro de Biotecnologia and the Centro de Química e Meio Ambiental IPEN/CNEN-SP. We also thank FAPESP for financial support (2010/52666-4).

## References

[1] M. West, J.B. Hedges, A. Chen, A.W. Johnson, Defining the order in which Nmd3p and RpL10p load onto nascent 60S ribosomal subunits, Mol. Cell. Biol. 25 (2005) 3802–3813.
[2] S.F. Dowdy, K.M. Lai, B.E. Weissman, Y. Matsui, B.L.M. Hogan, E.J. Stanbridge, The isolation and characterization of a novel cDNA demonstrating an altered mRNA level in nontumorigenic Wilms' microcell hybrid cells, Nucleic Acids Res. 19 (1991) 5763–5769.
[3] H. Inada, J. Mukai, S. Matsushina, T. Tanaka, QM is a novel Zinc-binding transcription regulatory proteins: its binding to c-jun is regulated by zinc ions and phosphorylation by protein kinase C, Biochem. Biophys. Res. Commun. 230 (1997) 331–334.
[4] I.G. Wool, Extraribosomal functions of ribosomal proteins, Trends Biochem. Sci. 21 (1996) 164–165.
[5] T.M. Loftus, Y.H. Nguyen, E.J. Stanbridge, The QM protein associates with ribosomes in the rough endoplasmic reticulum, Biochemistry – US 36 (1997) 8224–8230.
[6] I. Imafuku, T. Masaki, M. Waragai, S. Takeuchi, M. Kawabata, S. Hirai, S. Ohno, L.E. Nee, C.F. Lippa, I. Kanazawa, M. Imagawa, H. Okazawa, Presenilin 1 suppress the function of c-Jun homodimers via interaction with QM/Jif-1, J. Cell Biol. 147 (1999) 121–133.
[7] H.S. Oh, H. Kwon, S.K. Sun, C.H. Yang, QM, a putative tumor suppressor, regulates proto-oncogene c-Yes, J. Biol. Chem. 277 (2000) 36489–36498.
[8] R.J.R. Roskoski, Src protein-tyrosine kinase structure and regulation, Biochem. Biophys. Res. Commun. 324 (2004) 1155–1164.
[9] G. Altinok, I.J. Powel, M. Che, K. Hormont, F.H. Sarkar, W.A. Sakr, D. Grignon, D.J. Liao, Reduction of QM protein expression correlates with tumor grade in prostatic adenocarcinoma, Prostate Cancer P.D. 9 (2006) 77–82.
[10] X.J. Shen, R. Ali-Fehmi, C.R. Weng, F.H. Sarker, D. Grignon, D.J. Liao, Loss of heterozygosity and microsatellite instability all the Xq28 and the A/G heterozygoty of the QM gene are associated with ovarian cancer, Cancer Biol. Ther. 5 (2006) 523–528.
[11] X. Gong, R. Delorme, F. Fauchereau, C.M. Durand, P. Chaste, C. Betancur, H. Goubran-Botros, G. Nygren, H. Anckarsäter, M. Rastam, I.C. Gillberg, S. Kopp, M.C. Mouren-Simeoni, C. Gillberg, M. Leboyer, T. Bourgeron, An investigation of ribosomal protein L10 gene in autism spectrum disorders, BMC Med. Genet. 10 (2009) 1–5.
[12] A. Chiocchetti, G. Pakalapati, E. Duketis, S. Wiemann, A. Poustka, F. Poustka, S.M. Klauck, Mutation and expression analyses of the ribosomal protein gene RPL10 in an extended German sample of patients with autism spectrum disorder, Am. J. Med. Genet. A. 155A (2011) 1472–1475.
[13] A.M. Massad-Costa, I.D.C. Da Silva, R. Affonso, J.M. Soares, M.G. Nunes, G.R. De Lima, E.C. Baracat, Gene analysis in patients with premature ovarian failure or gonadal dysgenesis: a preliminary study, Maturitas 57 (2007) 399–404.
[14] M. Nishimura, T. Kaminishi, C. Takemoto, M. Kawazoe, T. Yoshida, A. Tanaka, S. Sugano, M. Shirouzu, T. Ohkubo, S. Yokoyama, Y. Kobayashi, Crystal structure of human ribosomal protein L10 core domain reveals eukaryote-specific motifs in addition to the conserved fold, J. Mol. Biol. 377 (2008) 421–430.
[15] M. Nishimura, T. Kaminishi, M. Kawazoe, M. Shirouzu, C. Takemoto, S. Yokoyama, A. Tanaka, S. Sugano, T. Yoshida, T. Ohkubo, Y. Kobayashi, Purification, crystallization and preliminary X-ray diffraction study of human ribosomal protein L10 core domain, Acta Crystallogr. F 63 (2007) 950–952.
[16] E. Garcıa-Fruitos, E. Vazquez, C. Dıez-Gil, J.L. Corchero, J. Seras-Franzoso, I. Ratera, J. Veciana, A. Villaverde, Bacterial inclusion bodies: making gold from waste, Trends Biotechnol. 30 (2012) 65–70.
[17] S. Peternel, J. Grdadolnik, V. Gaberc-Porekar, R. Komel, Engineering inclusion bodies for non denaturing extraction of functional proteins, Microb. Cell Fact. 7 (2008) 1–9.
[18] C.V. Carvalho, G. Ricci, R. Affonso, Guia de práticas em Biologia Molecular, first ed., Yends, São Paulo, 2010.
[19] M. Pereira, Clonagem, expressão, purificação e caracterização estrutural da proteína ribossomal L10 humana recombinante (Master's degree), Nuclear and Energy Research Institute, 2009.
[20] U.K. Laemmli, Cleavage of structural proteins during the assembly of the head of bacteriophage T4, Nature 227 (1970) 680–685.
[21] W.N. Burnertte, "Western blotting": electrophoretic transfer of proteins form sodium dodecyl sulfate–polyacrylamide gels to unmodified nitrocellulose and radiographic detection with antibody and radioiodinate protein A, Anal. Biochem. 112 (1981) 195–203.
[22] M.M. Bradford, A rapid and sensitive method for the quantitation of microgram quantities of protein utilizing the principle of protein-dyue binding, Anal. Biochem. 72 (1976) 248–254.
[23] G. Bohm, R. Muhr, R. Jaenicke, Quantitative analysis of protein far UV circular dichroism spectra by neural networks, Protein Eng. 5 (1992) 191–195.
[24] J.E. Oliveira, C.R. Soares, C. Peroni, E. Gimbo, I.M.C. Camargo, L. Morganti, M.H. Bellini, R. Affonso, R. Rarkaten, P. Bartolini, M.T.C.P. Ribela, High-yield purification of biosynthetic human growth hormone secreted in *E. coli* periplasmic space, J. Chromatogr. 852 (1999) 441–450.
[25] A. Schrödel, A. Marco, Characterization of the aggregates formed during recombinant protein expression in bacteria, BMC Biochem. 6 (2005) 1–11.
[26] R.W. Graham, J.M. Greenwood, R.A.A. Warren, D.G. Kilburn, D.E. Trimbur, The pTug A and pTug as vectors for the high-level expression of cloned genes in *Escherichia coli*, Gene 158 (1995) 51–54.
[27] J.A. Chesshyre, A.R. Hipkiss, Low temperatures stabilize interferon a-2 against proteolysis in methylophilus methylotrophus and *Escherichia coli*, Appl. Microbiol. Biotechnol. 31 (1989) 158–162.
[28] P.H. Sørensen, K.K. Mortensen, Soluble expression of recombinant proteins in the cytoplasm of *Escherichia coli*, Microb. Cell Fact. 4 (1) (2005) 1–8.
[29] A. Vera, N. González-Montalbán, A. Arís, A. Villaverde, The conformational quality of insoluble recombinant proteins is enhanced at low growth temperatures, Biotechnol. Bioeng. 96 (2007) 1101–1106.
[30] A.P. Demchenko, Fluorescence and dynamics in proteins, Top. Fluoresc. Spectrosc. 3 (2002) 65–111.
[31] Y. Zhang, J. Hunag, Q. Meng, T. Jiang, L. Xie, Z. Wang, R. Zhang, Molecular cloning and expression of pearl oyster (*Pincatada fucata*) homologue of mammalian putative tumor suppressor QM, Mar. Biotechnol. 6 (2004) 8–16.
[32] K.L.B. Borden, Ring fingers and B-boxes: zinc-binding protein–protein interaction domains, Biochem. Cell Biol. 76 (1998) 351–358.
[33] B.A. Van der Reijden, C.A.J. Erpelinck-Verschueren, B. Löwenberg, J.H. Jansentriad, Triads: a new class of proteins with a novel cysteine-rich signature, Protein Sci. 8 (1999) 1557–1561.